Eur. Phys. J. C (2024) 84:61
https://doi.org/10.1140/epjc/s10052-023-12362-5

THE EUROPEAN PHYSICAL JOURNAL C

Regular Article - Theoretical Physics

Pair production of the singlet vector-like B quark at the CLIC

Jin-Zhong Han[1,a], **Yao-Bei Liu**[2,b], **Shi-Yu Xu**[1]

[1] School of Physics and Telecommunications Engineering, Zhoukou Normal University, Zhoukou 466001, People's Republic of China
[2] Henan Institute of Science and Technology, Xinxiang 453003, People's Republic of China

Received: 9 July 2023 / Accepted: 15 December 2023 / Published online: 20 January 2024

Abstract Vector-like quarks (VLQs) are a common feature of many scenarios of new physics beyond the Standard Model (SM), which generally decay into a SM third-generation quark with a SM gauge boson or a Higgs boson. The presence of a new exotic decay mode of VLQs will reduce the branching ratios of these standard decay modes and thus relax the current mass exclusion limits from LHC experiments. Based on a model-independent framework, we investigate the prospect of discovering the pair production of the weak-singlet VLQ-B at the future 3-TeV Compact Linear Collider (CLIC), by focusing on the final states including one Z boson and four b-jets via two types of modes: $Z \to \ell^+\ell^-$ and $Z \to \nu\bar{\nu}$. By performing a rapid detector simulation of the signal and background events, and considering the initial state radiation and beamstrahlung effects, the exclusion limit at the 95% confidence level and the 5σ discovery prospects are respectively obtained on the branching ratio of $B \to bZ$ and the VLQ-B masses at the future 3-TeV CLIC with an integrated luminosity of 5 ab^{-1}.

1 Introduction

New heavy quarks appear in a variety of new physics models beyond the Standard Model (SM), formulated to obtain an answer to the problem of the naturalness of the electroweak (EW) scale [1–9]. Vector-like quarks (VLQs) are spin 1/2 particles characterized by having left- and right-handed components defined by the same color and EW quantum numbers [10], and thus could still be viable under the present searches. However, an extra fourth generation of SM-like quarks [11,12] should be much heavier due to the EW precision constraints, and thus a certain non-perturbative method is needed to reliably analyze the strongly coupled Yukawa sector of these extra heavy chiral quarks. VLQs can have different charge assignments under the SM EW gauge group $SU(2)_L \times U(1)_Y$. Hence, there exists the possibility of having multiple VLQs, including electroweak singlet $[T, B]$, electroweak doublets $[(X, T), (T, B)$ or $(B, Y)]$, or electroweak triplets $[(X, T, B)$ or $(T, B, Y)]$. It is generally assumed that the VLQs decay into a SM third-generation quark with a SM gauge boson or a Higgs boson, therefore providing a rich phenomenology at future high-energy colliders [13–35].

For a vector-like B-quark (VLQ-B) with electric charge $-(1/3)$e, direct searches generally assume three standard decay channels: $B \to tW$, bZ, and bH. Very recently, ATLAS and CMS collaborations have focused primarily on the quantum chromodynamics (QCD)-induced pair production modes of VLQs and have led to lower bounds on the VLQ masses of approximately 1–1.5 TeV [36–41]. Using Run 2 data with a total integrated luminosity of 137 fb^{-1}, the CMS Collaboration recently presented a search for VLQ-B pair production in the fully hadronic final state [40], and excluded their masses up to 1.57 and 1.39 TeV for 100% $B \to bh$ and 100% $B \to tZ$, respectively. The ATLAS Collaboration presented a search for the pair production of VLQs optimized for decays into a Z boson and a third-generation SM quark [42]. The lower limits on the masses of VLQ-B are 1.20 TeV for the weak-isospin singlet model and 1.42 TeV for 100% $B \to tZ$ cases. However, these bounds would be relaxed if such VLQs were to have non-standard decay channels. Recently, exotic decays of the VLQs in different set-ups with different collider signatures have been considered in the literature [43–57].

Compared with the complicated QCD background at the hadron colliders, the future high-energy linear e^+e^- collider is a precision machine with which the properties of such new VLQs can be measured precisely [58–61]. In particular, the final stage of the Compact Linear Collider (CLIC) will operate at energy of 3 TeV [62], and any such new particles

[a] e-mail: hanjinzhong@zknu.edu.cn
[b] e-mail: liuyaobei@hist.edu.cn (corresponding author)

can be produced with a sizable rate up to the kinematic limit of 1.5 TeV, and in some cases up to 3 TeV, via single production mechanisms [63]. Recently, the single production processes of VLQs at the CLIC have been widely studied via different decay modes [64–71]. Unlike the single production mode, the production of VLQ pairs is model-independent, i.e., their cross sections depend only on their masses [72]. In this paper we will focus on the illustrative examples of VLQ-B pairs interacting with the third generation of SM quarks, and we will analyze their pair production signatures via the standard decay channels $B \to bZ$ (bh) at the future 3-TeV CLIC. Furthermore, we will estimate the reach for discovering (or excluding) VLQ-B in which it is assumed that the exotic decay mode is possible and will take the branching ratio (BR) of $B \to bZ$ as a free parameter.

This paper is organized as follows: In Sect. 2, we briefly describe the couplings of the singlet VLQ-B with the SM particles in the simplified model and the direct LHC constraints on its mass and the branching ratio of $B \to bZ$. In Sect. 3, we discuss the pair production process at the 3-TeV CLIC, and perform a detailed collider analysis of the relevant signals and backgrounds. Finally, we provide a summary in Sect. 4.

2 Singlet VLQ-B in the simplified model

A generic parameterization of an effective Lagrangian for the singlet VLQ-B is given by [1]

$$\mathcal{L}_{\rm eff} = \frac{g\kappa_B}{\sqrt{2}}\left[\frac{1}{\sqrt{2}}\bar{B}_L W_\mu^+ \gamma^\mu t_L + \frac{1}{2c_W}\bar{B}_L Z_\mu \gamma^\mu b_L - \frac{m_B}{2m_W}\bar{B}_R h b_L - \frac{m_b}{2m_W}\bar{B}_L h b_R\right] - \frac{e}{6c_W}\{\bar{B}B_\mu\gamma^\mu B\} - \frac{e}{4s_W}\{\bar{B}W_\mu^3\gamma^\mu B\} + h.c., \quad (1)$$

where g is the $SU(2)_L$ gauge coupling constant, and there are two free parameters: the VLQ-B quark mass m_B and the coupling strength to SM quarks in units of standard couplings, κ_B.

Assuming an almost degenerate VLQ mass hierarchy, they are generally assumed to decay into a third-generation quark and either a W/Z boson or a Higgs boson. For a heavy weak-isospin singlet VLQ-B, the relationship of the BRs of three standard decay modes is

$$\mathrm{Br}(B \to tW) \approx 2\mathrm{Br}(B \to bZ) \approx 2\mathrm{Br}(B \to bh), \quad (2)$$

which is a good approximation as expected from the Goldstone boson equivalence theorem [73–77]. With the introduction of the new decay modes $B \to X$, the sum of the above three standard decay modes changes to

$$\mathrm{Br}(B \to bZ) + \mathrm{Br}(B \to bh) + \mathrm{Br}(B \to tW) = 1 - \beta_{\rm new}, \quad (3)$$

where $\beta_{\rm new}$ is the BR for the new exotic decay channel, such as $B \to bS$ (an additional scalar or pseudoscalar particle [56,57]). A smaller BR in the new mode $\beta_{\rm new}$ implies larger BRs in the SM modes. Based on Eqs. (2)–(3), we can obtain

$$\mathrm{Br}(B \to bZ) \simeq (1 - \beta_{\rm new})/4. \quad (4)$$

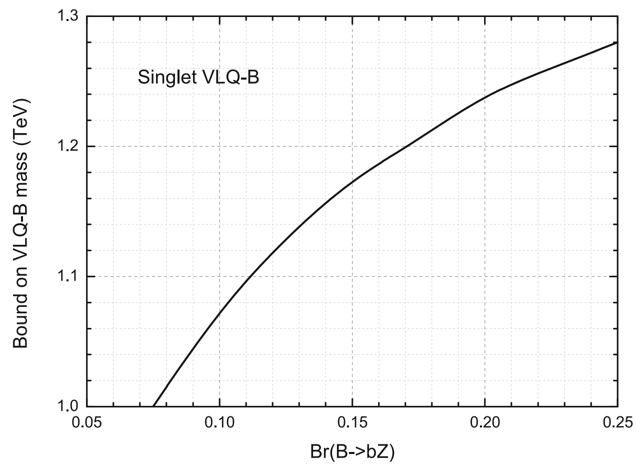

Fig. 1 LHC exclusion limits on the VLQ-B as a function of $\mathrm{Br}(B \to bZ)$ in the singlet B model including non-standard decay modes

In this case, it is instructive to analyze the current constraints from direct searches of VLQ-B. Very recently, Refs. [56, 57] recast the current LHC searches to put mass exclusion bounds on VLQ-B as a function of the branching ratio in the new decay mode. In Fig. 1, we show the exclusion mass limits on VLQ-B as a function of $\mathrm{Br}(B \to bZ)$ according to Eq. (4) and the results in the literature [56], where they recast the relevant limits from the available exclusive [39,40] and inclusive [41] searches to select the strongest one. From the rescaled VLQ-B limits in Fig. 1, one can see that the VLQ-B mass could be smaller than 1.3 TeV for the smaller BR of the standard decay mode $B \to bZ$, which implies that the VLQ-B could be pair-produced at the future 3-TeV CLIC.

3 Collider simulation and analysis

In order to make a prediction for the signal, we calculate the production cross section for the process $e^+e^- \to B\bar{B}$ at leading order (LO). Note that here the effects of initial state radiation (ISR) and beamstrahlung are also considered at the 3-TeV CLIC in MadGraph5_aMC_v3.3.2 [78] by adding the following commands in the run_card:

[1] Details are provided on the URL http://feynrules.irmp.ucl.ac.be/wiki/VLQ_bsingletvl.

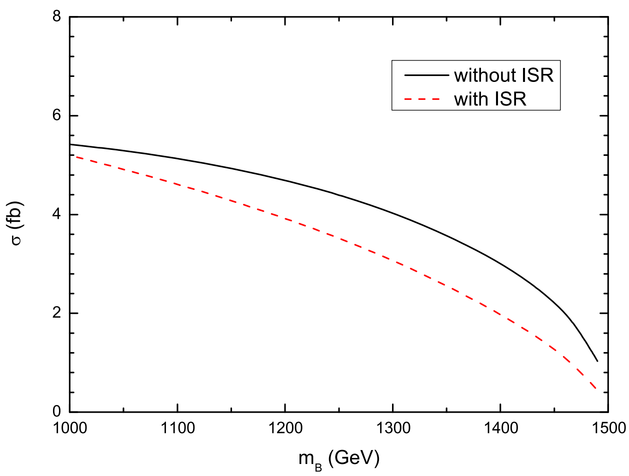

Fig. 2 Total cross section of σ as a function of m_B at the 3-TeV CLIC with and without ISR effects

```
set lpp1 +3
set lpp2 -3
set pdlabel clic3000ll
```

In Fig. 2, we show the dependence of the cross sections σ as a function of m_B with (without) ISR and beamstrahlung effects. One can see that the cross sections can be changed with ISR and beamstrahlung effects compared with those without ISR and beamstrahlung effects. In the region of $m_B \in$ [1000, 1490] GeV, the ratios of cross sections with and without ISR and beamstrahlung effects are changed from 0.96 to 0.43; thus, it is necessary to consider these effects at the future 3-TeV CLIC, especially for the high VLQ-B masses. For $m_B = 1.2$ (1.45) TeV, the cross section can reach about 3.94 (1.29) fb with ISR and beamstrahlung effects.

Under the narrow-width approximation (NWA), it is possible to separate and factorize production and decay of the heavy quarks, thus allowing for a model-independent analysis of the results [79]. For the processes $e^+e^- \to B\bar{B} \to bZ\bar{b}Z$ and $e^+e^- \to B\bar{B} \to bZ\bar{b}h$, their cross sections can be written as

$$\sigma_{bZbZ} \equiv \sigma_{e^+e^-\to B\bar{B}} \times \text{Br}(B \to bZ) \times \text{Br}(B \to bZ),$$
$$\sigma_{bZbh} \equiv \sigma_{e^+e^-\to B\bar{B}} \times \text{Br}(B \to bZ) \times \text{Br}(B \to bh).$$

Assuming the relationship of $\text{Br}(B \to bZ) \simeq \text{Br}(B \to bh)$, we will take $\text{Br}(B \to bZ)$ as a free parameter in the remainder of this article.

We demand that a pair-produced VLQ-B event should have at least one Z boson and four b-jets, with one pair of b-jets decaying from a Z boson or a Higgs boson,

$$e^+e^- \to B\bar{B} \to \begin{cases} (bZ)\ (\bar{b}Z) \\ (bZ)\ (\bar{b}h) \\ (bh)\ (\bar{b}Z) \end{cases} \to b\bar{b}b\bar{b}Z. \quad (5)$$

In the next section, we will perform the Monte Carlo simulation and explore the discovery potentiality of VLQ-B through the subsequent leptonic decay channel $Z \to \ell^+\ell^-$ and the invisible decay channel $Z \to \nu\bar{\nu}$, respectively. To generate events for each signal benchmark, we pick model parameters such that $\kappa_B = 0.1$ and $\text{Br}(B \to bZ) = 0.25$ while ensuring that the NWA remains valid for VLQ-B.

Monte Carlo event simulations for the signal and SM background are interfaced to Pythia 8.20 [80] for fragmentation and showering. All event samples are fed into the Delphes 3.4.2 program [81] with the CLIC detector card designed for 3 TeV [82]. In our analysis, jets are clustered with the Valencia Linear Collider (VLC) algorithm [83,84] in exclusive mode with a fixed number of jets ($N = 4$, where N corresponds to the number of partons expected in the final state) and fixed-size parameter $R = 0.7$. The b-tagging efficiency is taken as the loose working points with 90% b-tagging efficiency in order not to excessively reduce the signal efficiency. Finally, event analysis is performed by using MadAnalysis 5 [85].

3.1 The decay channel $Z \to \ell^+\ell^-$

In this subsection, we analyze the signal and background events at the 3-TeV CLIC through the $Z \to \ell^+\ell^-$ ($\ell = e, \mu$) decay channel:

$$e^+e^- \to B\bar{B} \to \begin{cases} (bZ)\ (\bar{b}Z) \\ (bZ)\ (\bar{b}h) \\ (bh)\ (\bar{b}Z) \end{cases} \to 4b + \ell^+\ell^-. \quad (6)$$

For this channel, the typical signal is two opposite-sign same-flavor (OSSF) leptons coming from one Z boson and four b-tagged jets, with a pair of b-tagged jets coming from a Z boson or a Higgs boson. The dominant SM backgrounds come from the SM processes $e^+e^- \to Zhb\bar{b}$ and $e^+e^- \to ZZb\bar{b}$. Note that the contributions from the processes $e^+e^- \to ZZh$, $e^+e^- \to ZZZ$, and $e^+e^- \to Zhh$ are also included with the decay modes $Z \to \ell^+\ell^-$, $Z \to b\bar{b}$, and $h \to b\bar{b}$.

To identify objects, we choose the basic cuts at parton level for the signals and SM backgrounds as follows:

$$p_T^{\ell/j/b} > 25\ \text{GeV}, \quad |\eta_{\ell/b/j}| < 2.5, \quad \Delta R_{ij} > 0.4, \quad (7)$$

where $\Delta R = \sqrt{\Delta\Phi^2 + \Delta\eta^2}$ denotes the separation in the rapidity-azimuth plane, and $p_T^{\ell,b,j}$ are the transverse momentum of leptons, b-jets, and light jets.

In Fig. 3, we plot differential distributions for signals and SM backgrounds including the invariant mass distribution for the Z boson ($M_{\ell_1\ell_2}$), the transverse momentum distributions of the leading and sub-leading leptons ($p_T^{\ell_1\ell_2}$), the transverse momentum distributions of the leading and sub-leading b-jets ($p_T^{b_1}$, $p_T^{b_2}$), the invariant mass distribution for the Z boson or Higgs boson ($M_{b_3b_4}$), and the separations $\Delta R_{b_3,b_4}$. For the

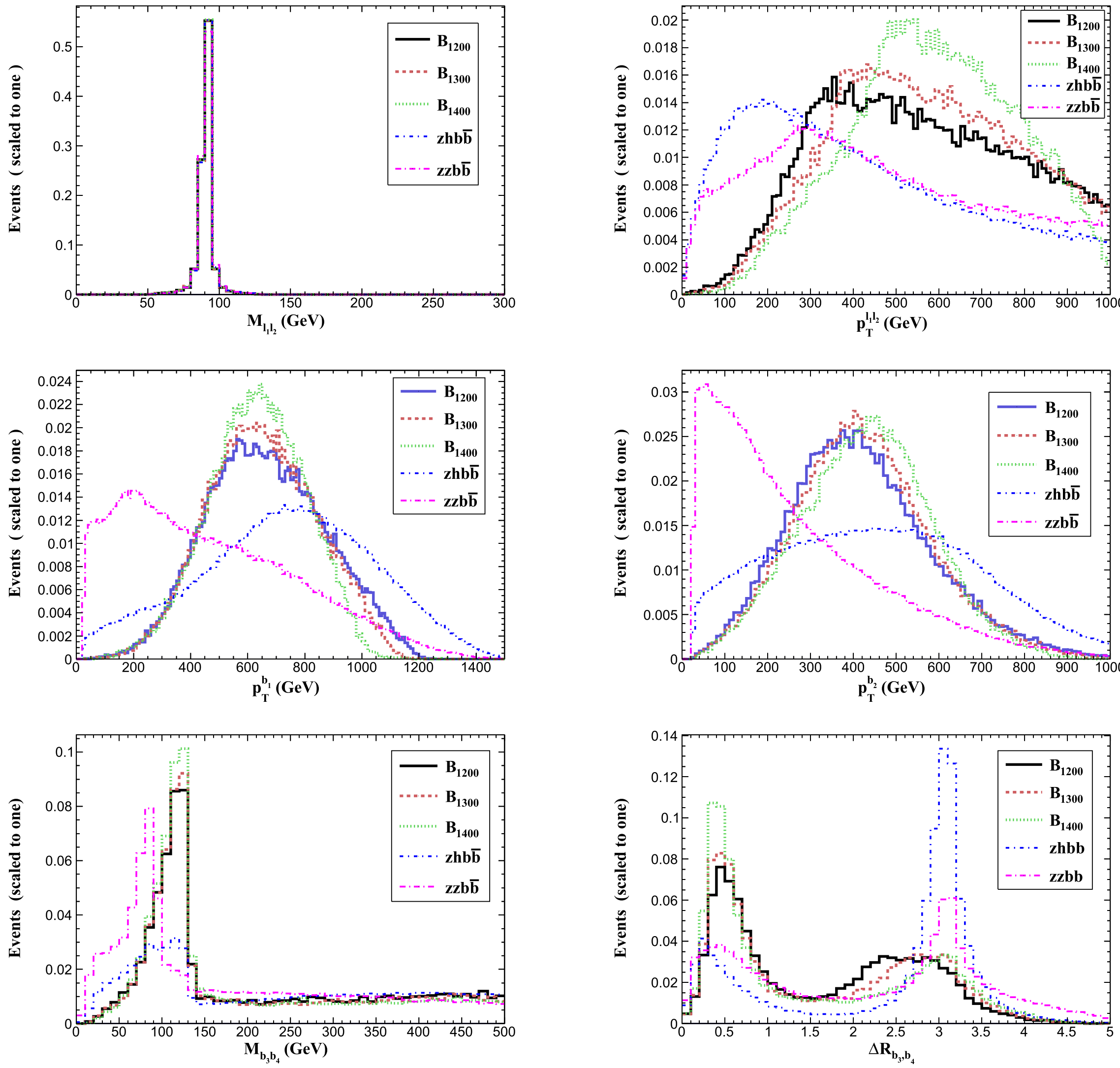

Fig. 3 Normalized distributions for the signals (with m_B = 1200, 1300, 1400 GeV) and SM backgrounds

signal, the leptons ℓ_1 and ℓ_2 are two OSSF leptons that are assumed to be the product of the Z boson decay, and at least two b-tagged jets are assumed to be the product of one Z boson or a Higgs boson decay. Based on these kinematic distributions, we can impose the following set of cuts:

- Cut-1: There are exactly two isolated leptons ($N(\ell) = 2$), and the invariant mass of the Z boson is required to have $|M_{\ell_1\ell_2} - m_Z| < 10$ GeV£¬ and the transverse momenta of two leptons are required $p_T^{\ell_1\ell_2} > 200$ GeV.
- Cut-2: There are exactly four b-tagged jets ($N(b) = 4$), and the transverse momenta of the leading and sub-leading b-jet are required $p_T^{b_1} > 400$ GeV and $p_T^{b_2} > 250$ GeV.
- Cut-3: The invariant masses of the Z boson or the Higgs boson are required to have 50 GeV $< M_{b_3b_4} <$ 150 GeV, with $\Delta R_{b_3,b_4} < 1$.

Table 1 Cut flow of the cross sections (in fb) for the signals with three typical VLQ-B quark masses and SM backgrounds

Cuts	Signals			Backgrounds	
	1200 GeV	1300 GeV	1400 GeV	$Zhb\bar{b}$	$ZZb\bar{b}$
Basic	0.031	0.024	0.015	0.005	0.004
Cut-1	0.023	0.018	0.012	0.0025	0.0021
Cut-2	0.012	0.009	0.006	0.0012	0.00055
Cut-3	0.0043	0.0036	0.0026	0.00026	0.00015

We present the cross sections of three typical signals (m_B = 1200, 1300, 1400 GeV) and the relevant backgrounds after imposing the cuts in Table 1. One can see that all the SM backgrounds are suppressed very efficiently, while the signals still have relatively good efficiency at the end of

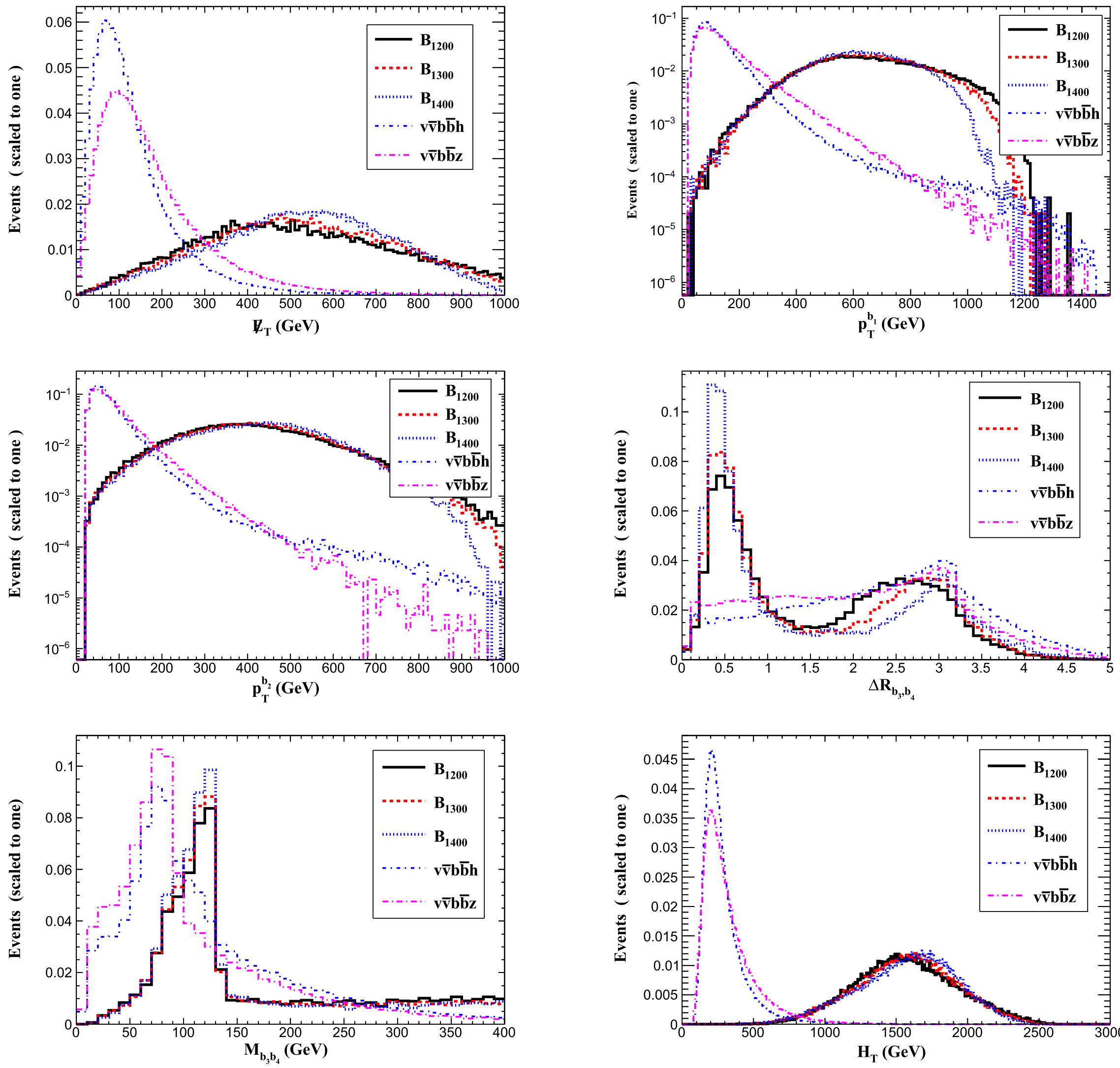

Fig. 4 Normalized distributions for the signals (with m_B = 1200, 1300, 1400 GeV) and SM backgrounds

the cut flow. The cross section of the total SM background is about 0.4×10^{-3} fb.

3.2 The decay channel $Z \to \nu\bar{\nu}$

In this subsection, we analyze the signal and background events through the decay channel of the invisible decays $Z \to \nu\bar{\nu}$:

$$e^+e^- \to B\bar{B} \to \begin{cases} (bZ)\ (\bar{b}Z) \\ (bZ)\ (\bar{b}h) \\ (bh)\ (\bar{b}Z) \end{cases} \to 4b + \not{E}_T. \tag{8}$$

For this channel, the main SM backgrounds come from the processes $e^+e^- \to \nu\bar{\nu}b\bar{b}Z$ and $e^+e^- \to \nu\bar{\nu}b\bar{b}h$ with the cross sections of 21.7 fb and 2.5 fb, respectively. Note that the contributions from the processes $e^+e^- \to Zhb\bar{b}$, $e^+e^- \to ZZb\bar{b}$, $e^+e^- \to Zhh$, $e^+e^- \to ZZh$, $e^+e^- \to ZZZ$, $e^+e^- \to \nu_e\bar{\nu}_e hh$, $e^+e^- \to \nu_e\bar{\nu}_e Zh$, and $e^+e^- \to \nu_e\bar{\nu}_e ZZ$ are also included with the decay modes $Z \to \nu\bar{\nu}$, $Z \to b\bar{b}$, and $h \to b\bar{b}$.

Obviously, the signal events should contain large missing transverse energy $\not{E}_T$ from the boosted Z boson. Furthermore, at least two b-tagged jets are coming from the Z boson or Higgs boson decay. In order to obtain some hint of further cuts for reducing the SM backgrounds, we analyzed the normalized distributions of the missing transverse energy $\not{E}_T$, the transverse momentum distributions of the leading and sub-leading b-jets $p_T^{b_1,b_2}$, the separations $\Delta R_{b_3,b_4}$, the invariant mass distribution $M_{b_3 b_4}$, and the scalar sum of the transverse energy of all final-state jets H_T for signals and SM backgrounds as shown in Fig. 4. Based on these kinematic distributions, a set of further cuts are given as:

Table 2 Cut flow of the cross sections (in fb) for the signals with three typical VLQ-B quark masses and SM backgrounds

Cuts	Signals			Backgrounds	
	1200 GeV	1300 GeV	1400 GeV	$\nu\bar{\nu}b\bar{b}h$	$\nu\bar{\nu}b\bar{b}Z$
Basic	0.093	0.071	0.044	2.44	4.51
Cut-1	0.085	0.066	0.042	0.44	1.36
Cut-2	0.016	0.013	0.0093	0.0044	0.011
Cut-3	0.015	0.013	0.0088	0.0019	0.0037

- Cut-1: The transverse missing energy is required $\not{E}_T > 200$ GeV.
- Cut-2: Any electrons and muons are forbidden ($N(\ell) = 0$), and there are exactly four b-tagged jets ($N(b) = 4$). Furthermore, the transverse momenta of the leading and sub-leading b-jets are required $p_T^{b_1} > 300$ GeV and $p_T^{b_2} > 150$ GeV. The invariant masses of the remaining two b-tagged jets are required to have 50 GeV $< M_{b_3 b_4} < 150$ GeV, with $\Delta R_{b_3, b_4} < 1$.
- Cut-3: The scalar sum of the transverse energy of all final-state jets $H_T > 1000$ GeV.

We summarize the cross sections of three typical signals ($m_B = 1200, 1300, 1400$ GeV) and the relevant backgrounds after imposing the cuts in Table 2. One can see that the total SM backgrounds are suppressed very efficiently, with a cross section of about 5.6×10^{-3} fb.

3.3 Discovery and exclusion significance

In order to analyze the observability, we use the median significance to estimate the expected discovery and exclusion significance [86]:

$$\mathcal{Z}_{\rm disc} = \sqrt{2\left[(s+b)\ln\left(\frac{(s+b)(1+\delta^2 b)}{b+\delta^2 b(s+b)}\right) - \frac{1}{\delta^2}\ln\left(1+\delta^2\frac{s}{1+\delta^2 b}\right)\right]}$$
$$\mathcal{Z}_{\rm excl} = \sqrt{2\left[s - b\ln\left(\frac{b+s+x}{2b}\right) - \frac{1}{\delta^2}\ln\left(\frac{b-s+x}{2b}\right)\right] - (b+s-x)\left(1+\frac{1}{\delta^2 b}\right)}, \quad (9)$$

where $x = \sqrt{(s+b)^2 - 4s\delta^2 b^2/(1+\delta^2 b)}$, s and b are the numbers of signal and background events at a given luminosity, respectively, and δ is the percentage systematic error on the SM background estimate. In the limit of $\delta \to 0$, these expressions can be simplified as

$$\mathcal{Z}_{\rm disc} = \sqrt{2[(s+b)\ln(1+s/b) - s]},$$
$$\mathcal{Z}_{\rm excl} = \sqrt{2[s - b\ln(1+s/b)]}. \quad (10)$$

It is instructive to acknowledge systematic uncertainties at the experiment which can effect our results. To show this, we include a 10% systematic uncertainty alongside the null systematic uncertainty results.

In Fig. 5, we plot the 95% CL exclusion limit and 5σ sensitivity reaches for Br($B \to bZ$) as a function of m_B at the 3-TeV CLIC with an integrated luminosity of 5 ab^{-1} for two decay channels with the aforementioned two systematic error cases of $\delta = 0$ and $\delta = 10\%$. We find that with a realistic 10% systematic error, the sensitivities are slightly weaker than those without any systematic error. For the $Z \to \ell^+\ell^-$ decay channel, the VLQ-B quark can be excluded in the region of Br($B \to bZ$) $\in [0.09, 0.27]$ and $m_B \in [1000, 1490]$ GeV at the 3-TeV CLIC with an integrated luminosity of 5 ab^{-1}, while the discover region can reach Br($B \to bZ$) $\in [0.16, 0.25]$ and $m_B \in [1000, 1420]$ GeV. For the $Z \to \nu\bar{\nu}$ decay channel, the VLQ-B quark can be excluded in the region of Br($B \to bZ$) $\in [0.09, 0.24]$ and $m_B \in [1000, 1490]$ GeV, and the discover region can reach Br($B \to bZ$) $\in [0.165, 0.25]$ and $m_B \in [1000, 1430]$ GeV at the 3-TeV CLIC with an integrated luminosity of 5 ab^{-1} (Fig. 6).

Next, we combine the significance with $\mathcal{Z}_{\rm comb} = \sqrt{\mathcal{Z}^2_{\ell\bar{\ell}} + \mathcal{Z}^2_{\nu\bar{\nu}}}$ by using the results from the above two decay channels with $\delta = 10\%$. One can see that the singlet VLQ-B can be excluded in the regions of Br($B \to bZ$) $\in [0.073, 0.21]$ and $m_B \in [1000, 1490]$ GeV at the 3-TeV CLIC with integrated luminosity of 5 ab^{-1}, while the discover regions can reach Br($B \to bZ$) $\in [0.13, 0.23]$ and $m_B \in [1000, 1450]$ GeV. For comparison, we also present the observed 95% CL exclusion limits at the 13-TeV LHC and the predicted exclusions at the future HL-LHC with an integrated luminosity of 3000 fb^{-1}. For simplicity, the exclusion limits for the HL-LHC are obtained by scaling the current LHC limits with the increased luminosity. We can observe that the future CLIC with $\sqrt{s} = 3$ TeV and an integrated luminosity of 5 ab^{-1} could provide better sensitivity than that reported in current experimental searches, and even better sensitivity than the future HL-LHC in some mass regions of VLQ-B (e.g., 1200–1500 GeV).

4 Conclusion

In this work, we have concentrated on the pair production of the singlet VLQ-B at the future 3-TeV CLIC in a simplified model. With the increasing branching in the extra decay mode, the existing limits on VLQs can be relaxed, so we

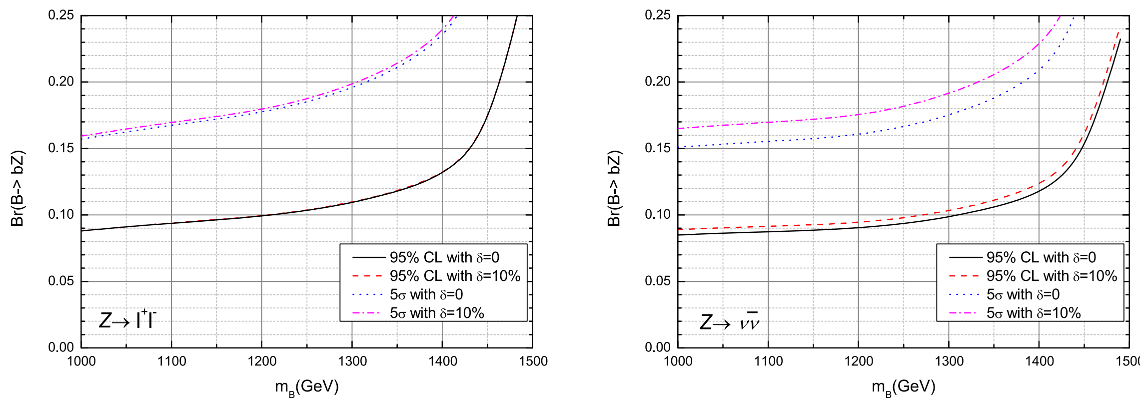

Fig. 5 Exclusion limit (at 95% CL) and discovery prospects (at 5σ) contour plots for the $Z \to \ell^+\ell^-$ decay channel (left), and for $Z \to \nu\bar{\nu}$ decay channel (right) in the $\mathrm{Br}(B \to bZ) - m_B$ planes at the future 3-TeV CLIC with an integrated luminosity of 5 ab^{-1}

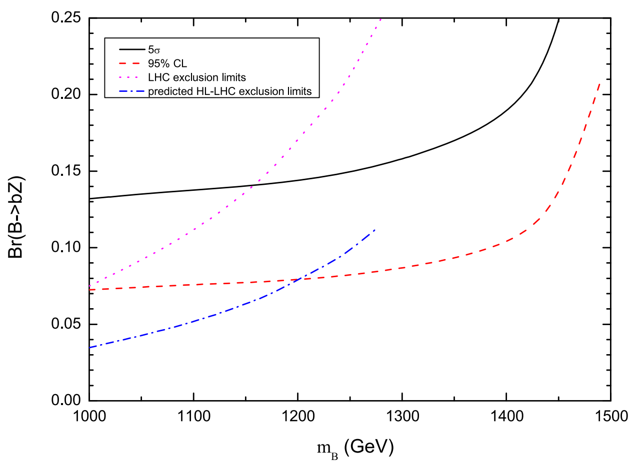

Fig. 6 Combined exclusion limit (at 95% CL) and discovery prospects (at 5σ) contour plots for the signal in $\mathrm{Br}(B \to bZ) - m_B$ planes at the 3-TeV CLIC with an integrated luminosity of 5 ab^{-1} with $\delta = 10\%$

first reinterpret the latest mass-exclusion limits for VLQ-B in terms of $\mathrm{Br}(B \to bZ)$. Then we perform a full simulation for the signals and the relevant SM backgrounds on the final states including one Z boson and four b-jets via two types of modes: $Z \to \ell^+\ell^-$ and $Z \to \nu\bar{\nu}$. We present the 95% CL exclusion limits and 5σ discovery prospects in the parameter plane of the two variables $\mathrm{Br}(B \to bZ)$ and the VLQ-B masses at the future 3-TeV CLIC with an integrated luminosity of 5 ab^{-1}. The results show that the VLQ-B quark can be excluded in the region of $\mathrm{Br}(B \to bZ) \in [0.073, 0.21]$ and $m_B \in [1000, 1490]$ GeV at the 3-TeV CLIC with integrated luminosity of 5 ab^{-1}, while the discover region can reach $\mathrm{Br}(B \to bZ) \in [0.13, 0.23]$ and $m_B \in [1000, 1450]$ GeV. We therefore expect that the signatures studied here will provide complementary information for detecting such VLQ-B, including non-standard decay modes, at the future 3-TeV CLIC.

Acknowledgements The work is supported by the Project of Innovation and Entrepreneurship Training for College Students in Henan Province (202310478033).

Data Availability Statement This manuscript has no associated data or the data will not be deposited. [Authors' comment: All relative data and results are displayed in the appropriate tables, there is no extra data to deposit.]

Funded by SCOAP^3.

References

1. A. De Simone, O. Matsedonskyi, R. Rattazzi, A. Wulzer, JHEP **04**, 004 (2013). https://doi.org/10.1007/JHEP04(2013)004
2. N. Arkani-Hamed, A.G. Cohen, E. Katz, A.E. Nelson, JHEP **07**, 034 (2002). https://doi.org/10.1088/1126-6708/2002/07/034
3. T. Han, H.E. Logan, B. McElrath, L.T. Wang, Phys. Rev. D **67**, 095004 (2003). https://doi.org/10.1103/PhysRevD.67.095004
4. S. Chang, H.J. He, Phys. Lett. B **586**, 95–105 (2004). https://doi.org/10.1016/j.physletb.2004.02.027
5. K. Agashe, R. Contino, A. Pomarol, Nucl. Phys. B **719**, 165 (2005). https://doi.org/10.1016/j.nuclphysb.2005.04.035
6. H.J. He, T.M.P. Tait, C.P. Yuan, Phys. Rev. D **62**, 011702(R) (2000). https://doi.org/10.1103/PhysRevD.62.011702
7. X.F. Wang, C. Du, H.J. He, Phys. Lett. B **723**, 314 (2013). https://doi.org/10.1016/j.physletb.2013.05.015
8. H.J. He, C.T. Hill, T.M.P. Tait, Phys. Rev. D **65**, 055006 (2002). https://doi.org/10.1103/PhysRevD.65.055006
9. H.J. He, Z.Z. Xianyu, J. Cosmol. Astropart. Phys. **10**, 019 (2014). https://doi.org/10.1088/1475-7516/2014/10/019

10. J.A. Aguilar-Saavedra, R. Benbrik, S. Heinemeyer, M. Pérez-Victoria, Phys. Rev. D **88**, 094010 (2013). https://doi.org/10.1103/PhysRevD.88.094010
11. H.J. He, N. Polonsky, Sf. Su, Phys. Rev. D **64**, 053004 (2001). https://doi.org/10.1103/PhysRevD.64.053004
12. N. Chen, H.J. He, JHEP **04**, 062 (2012). https://doi.org/10.1007/JHEP04(2012)062
13. A. Atre, G. Azuelos, M. Carena, T. Han, E. Ozcan, J. Santiago, G. Unel, JHEP **08**, 080 (2011). https://doi.org/10.1007/JHEP08(2011)080
14. G. Cacciapaglia, A. Deandrea, L. Panizzi, N. Gaur, D. Harada, Y. Okada, JHEP **03**, 070 (2012). https://doi.org/10.1007/JHEP03(2012)070
15. J.W. Nutter, R. Schwienhorst, D.G.E. Walker, J.H. Yu, Phys. Rev. D **86**, 094006 (2012). https://doi.org/10.1103/PhysRevD.86.094006
16. Y. Okada, L. Panizzi, Adv. High Energy Phys. **2013**, 364936 (2013). https://doi.org/10.1155/2013/364936
17. M. Buchkremer, G. Cacciapaglia, A. Deandrea, L. Panizzi, Nucl. Phys. B **876**, 376–417 (2013). https://doi.org/10.1016/j.nuclphysb.2013.08.010
18. S. Yang, J. Jiang, Q.S. Yan, X. Zhao, JHEP **09**, 035 (2014). https://doi.org/10.1007/JHEP09(2014)035
19. O. Matsedonskyi, G. Panico, A. Wulzer, JHEP **12**, 097 (2014). https://doi.org/10.1007/JHEP12(2014)097
20. M. Backović, T. Flacke, S.J. Lee, G. Perez, JHEP **09**, 022 (2015). https://doi.org/10.1007/JHEP09(2015)022
21. D. Barducci, L. Panizzi, JHEP **12**, 057 (2017). https://doi.org/10.1007/JHEP12(2017)057
22. G. Cacciapaglia, A. Deandrea, N. Gaur, D. Harada, Y. Okada, L. Panizzi, JHEP **11**, 055 (2018). https://doi.org/10.1007/JHEP11(2018)055
23. G. Cacciapaglia, A. Carvalho, A. Deandrea, T. Flacke, B. Fuks, D. Majumder, L. Panizzi, H.S. Shao, Phys. Lett. B **793**, 206 (2019). https://doi.org/10.1016/j.physletb.2019.04.056
24. Y.B. Liu, Y.Q. Li, Eur. Phys. J. C **77**, 654 (2017). https://doi.org/10.1140/epjc/s10052-017-5228-4
25. S. Moretti, D. O'Brien, L. Panizzi, H. Prager, Phys. Rev. D **96**, 035033 (2017). https://doi.org/10.1103/PhysRevD.96.035033
26. Y.B. Liu, S. Moretti, Phys. Rev. D **100**, 015025 (2019). https://doi.org/10.1103/PhysRevD.100.015025
27. A. Buckley, J.M. Butterworth, L. Corpe, D. Huang, P. Sun, SciPost Phys. **9**, 069 (2020). https://doi.org/10.21468/SciPostPhys.9.5.069
28. A. Deandrea, T. Flacke, B. Fuks, L. Panizzi, H.S. Shao, JHEP **08**, 107 (2021). https://doi.org/10.1007/JHEP08(2021)107
29. X.Y. Tian, L.F. Du, Y.B. Liu, Nucl. Phys. B **965**, 115358 (2021). https://doi.org/10.1016/j.nuclphysb.2021.115358
30. X.Y. Tian, L.F. Du, Y.B. Liu, Eur. Phys. J. C **81**, 594 (2021). https://doi.org/10.1140/epjc/s10052-021-09385-1
31. B. Yang, M. Wang, H. Bi, L. Shang, Phys. Rev. D **103**, 036006 (2021). https://doi.org/10.1103/PhysRevD.103.036006
32. J.Z. Han, J. Yang, S. Xu, H.K. Wang, Nucl. Phys. B **975**, 115672 (2022). https://doi.org/10.1016/j.nuclphysb.2022.115672
33. J.Z. Han, Y.B. Liu, L. Xing, S. Xu, Chin. Phys. C **46**, 103103 (2022). https://doi.org/10.1088/1674-1137/ac79ab
34. J.Z. Han, S. Xu, W.J. Mao, H.Q. Song, Nucl. Phys. B **992**, 116235 (2023). https://doi.org/10.1016/j.nuclphysb.2023.116235
35. J.M. Alves, G.C. Branco, A.L. Cherchiglia, J.T. Penedo, P.M.F. Pereira, C.C. Nishi, M.N. Rebelo, J.I. Silva-Marcos, arXiv:2304.10561 [hep-ph]
36. M. Aaboud et al. [ATLAS], Phys. Rev. D **98**(11), 112010 (2018). https://doi.org/10.1103/PhysRevD.98.112010
37. M. Aaboud et al. [ATLAS], Phys. Rev. Lett. **121**(21), 211801 (2018). https://doi.org/10.1103/PhysRevLett.121.211801
38. A.M. Sirunyan et al. [CMS], JHEP **08**, 177 (2018). https://doi.org/10.1007/JHEP08(2018)177
39. A.M. Sirunyan et al. [CMS], Phys. Rev. D **100**(7), 072001 (2019). https://doi.org/10.1103/PhysRevD.100.072001
40. A.M. Sirunyan et al. [CMS], Phys. Rev. D **102**, 112004 (2020). https://doi.org/10.1103/PhysRevD.102.112004
41. [ATLAS], ATLAS-CONF-2021-024
42. G. Aad *et al*. [ATLAS], Phys. Lett. B **843**, 138019 (2023) https://doi.org/10.1016/j.physletb.2023.138019 [arXiv:2210.15413 [hep-ex]]
43. J.A. Aguilar-Saavedra, D.E. López-Fogliani, C. Muñoz, JHEP **06**, 095 (2017). https://doi.org/10.1007/JHEP06(2017)095
44. K. Das, T. Mondal, S.K. Rai, Phys. Rev. D **99**, 115002 (2019). https://doi.org/10.1103/PhysRevD.99.115002
45. R. Benbrik, E.B. Kuutmann, D. Buarque Franzosi, V. Ellajosyula, R. Enberg, G. Ferretti, M. Isacson, Y.B. Liu, T. Mandal, T. Mathisen et al., JHEP **05**, 028 (2020). https://doi.org/10.1007/JHEP05(2020)028
46. G. Cacciapaglia, T. Flacke, M. Park, M. Zhang, Phys. Lett. B **798**, 135015 (2019). https://doi.org/10.1016/j.physletb.2019.135015
47. J.A. Aguilar-Saavedra, J. Alonso-González, L. Merlo, J.M. No, Phys. Rev. D **101**, 035015 (2020). https://doi.org/10.1103/PhysRevD.101.035015
48. H. Zhou, N. Liu, Phys. Rev. D **101**, 115028 (2020). https://doi.org/10.1103/PhysRevD.101.115028
49. D. Wang, L. Wu, M. Zhang, Phys. Rev. D **103**, 115017 (2021). https://doi.org/10.1103/PhysRevD.103.115017
50. G. Corcella, A. Costantini, M. Ghezzi, L. Panizzi, G.M. Pruna, J. Šalko, JHEP **10**, 108 (2021). https://doi.org/10.1007/JHEP10(2021)108
51. G. Cacciapaglia, T. Flacke, M. Kunkel, W. Porod, JHEP **02**, 208 (2022). https://doi.org/10.1007/JHEP02(2022)208
52. X.M. Cui, Y.Q. Li, Y.B. Liu, Phys. Rev. D **106**, 115025 (2022). https://doi.org/10.1103/PhysRevD.106.115025
53. A. Banerjee, D.B. Franzosi, G. Ferretti, JHEP **03**, 200 (2022). https://doi.org/10.1007/JHEP03(2022)200
54. A. Banerjee, D.B. Franzosi, G. Cacciapaglia, A. Deandrea, G. Ferretti, T. Flacke, B. Fuks, M. Kunkel, L. Panizzi, W. Porod et al., arXiv:2203.07270 [hep-ph]
55. A. Bhardwaj, K. Bhide, T. Mandal, S. Mitra, C. Neeraj, Phys. Rev. D **106**(7), 075024 (2022). https://doi.org/10.1103/PhysRevD.106.075024
56. A. Bhardwaj, T. Mandal, S. Mitra, C. Neeraj, Phys. Rev. D **106**(9), 095014 (2022). https://doi.org/10.1103/PhysRevD.106.095014
57. J. Bardhan, T. Mandal, S. Mitra, C. Neeraj, Phys. Rev. D **107**(11), 115001 (2023). https://doi.org/10.1103/PhysRevD.107.115001
58. K. Kong, S.C. Park, JHEP **08**, 038 (2007). https://doi.org/10.1088/1126-6708/2007/08/038
59. A. Senol, A.T. Tasci, F. Ustabas, Nucl. Phys. B **851**, 289–297 (2011). https://doi.org/10.1016/j.nuclphysb.2011.05.022
60. L. Guo, W. Liu, W.G. Ma, R.Y. Zhang, W.J. Zhang, M.A. B, Commun. Theor. Phys. **62**, 824–832 (2014). https://doi.org/10.1088/0253-6102/62/6/09
61. Y.B. Liu, Z.J. Xiao, Nucl. Phys. B **892**, 63–82 (2015). https://doi.org/10.1016/j.nuclphysb.2014.12.027
62. H. Abramowicz et al. [CLIC Detector and Physics Study], arXiv:1307.5288 [hep-ex]
63. R. Franceschini, Int. J. Mod. Phys. A **35**, 2041015 (2020). https://doi.org/10.1142/S0217751X20410158
64. X. Qin, J.F. Shen, Nucl. Phys. B **966**, 115388 (2021). https://doi.org/10.1016/j.nuclphysb.2021.115388
65. L. Han, J.F. Shen, Eur. Phys. J. C **81**(5), 463 (2021). https://doi.org/10.1140/epjc/s10052-021-09245-y
66. J.Z. Han, J. Yang, S. Xu, H.K. Wang, Phys. Rev. D **105**, 015005 (2022). https://doi.org/10.1103/PhysRevD.105.015005
67. X. Qin, L.F. Du, J.F. Shen, Nucl. Phys. B **979**, 115784 (2022). https://doi.org/10.1016/j.nuclphysb.2022.115784

68. L. Han, L.F. Du, Y.B. Liu, Phys. Rev. D **105**, 115032 (2022). https://doi.org/10.1103/PhysRevD.105.115032
69. L. Han, J.F. Shen, Y.B. Liu, Eur. Phys. J. C **82**, 637 (2022). https://doi.org/10.1140/epjc/s10052-022-10527-2
70. J.Z. Han, S. Xu, H.Q. Song, Y.J. Wang, Nucl. Phys. B **985**, 116030 (2022). https://doi.org/10.1016/j.nuclphysb.2022.116030
71. B. Yang, S. Wang, X. Sima, L. Shang, Commun. Theor. Phys. **75**, 035202 (2023). https://doi.org/10.1088/1572-9494/acb9e3
72. X. Qin, C. Wang, Nucl. Phys. B **992**, 116248 (2023). https://doi.org/10.1016/j.nuclphysb.2023.116248
73. H.J. He, Y.P. Kuang, X.Y. Li, Phys. Rev. Lett. **69**, 2619 (1992). https://doi.org/10.1103/PhysRevLett.69.2619
74. H.J. He, Y.P. Kuang, X.Y. Li, Phys. Rev. D **49**, 4842 (1994). https://doi.org/10.1103/PhysRevD.49.4842
75. H.J. He, Y.P. Kuang, C.P. Yuan, Phys. Rev. D **51**, 6463 (1995). https://doi.org/10.1103/PhysRevD.51.6463
76. H.J. He, Y.P. Kuang, C.P. Yuan, Phys. Rev. D **55**, 3038 (1997). https://doi.org/10.1103/PhysRevD.55.3038
77. H.J. He, W.B. Kilgore, Phys. Rev. D **55**, 1515 (1997). https://doi.org/10.1103/PhysRevD.55.1515
78. J. Alwall, R. Frederix, S. Frixione, V. Hirschi, F. Maltoni, O. Mattelaer, H.-S. Shao, T. Stelzer, P. Torrielli, M. Zaro, JHEP **07**, 079 (2014). https://doi.org/10.1007/JHEP07(2014)079
79. S. Moretti, D. O'Brien, L. Panizzi, H. Prager, Phys. Rev. D **96**, 075035 (2017). https://doi.org/10.1103/PhysRevD.96.075035
80. T. Sjöstrand, S. Ask, J.R. Christiansen et al., Comput. Phys. Commun. **191**, 159 (2015). https://doi.org/10.1016/j.cpc.2015.01.024
81. J. de Favereau et al. (DELPHES 3 Collaboration), JHEP **02**, 057 (2014). https://doi.org/10.1007/JHEP02(2014)057
82. E. Leogrande, P. Roloff, U. Schnoor, M. Weber, arXiv:1909.12728 [hep-ex]
83. M. Boronat, J. Fuster, I. Garcia, E. Ros, M. Vos, Phys. Lett. B **750**, 95–99 (2015). https://doi.org/10.1016/j.physletb.2015.08.055
84. M. Boronat, J. Fuster, I. Garcia, P. Roloff, R. Simoniello, M. Vos, Eur. Phys. J. C **78**, 144 (2018). https://doi.org/10.1140/epjc/s10052-018-5594-6
85. E. Conte, B. Fuks, G. Serret, Comput. Phys. Commun. **184**, 222 (2013). https://doi.org/10.1016/j.cpc.2012.09.009
86. G. Cowan, K. Cranmer, E. Gross, O. Vitells, Eur. Phys. J. C **71**, 1554 (2011). https://doi.org/10.1140/epjc/s10052-011-1554-0. [erratum: Eur. Phys. J. C 73, 2501 (2013)]